

Metabolism of oxysterols derived from nonenzymatic oxidation of 7-dehydrocholesterol in cells^S

Libin Xu,^{1,*} Zeljka Korade,[†] Dale A. Rosado, Jr.,^{2,*} Karoly Mirnics,[†] and Ned A. Porter^{1,*}

Department of Chemistry and Vanderbilt Institute of Chemical Biology* and Department of Psychiatry and Vanderbilt Kennedy Center for Research on Human Development,[†] Vanderbilt University, Nashville, TN 37235

Abstract Recent studies suggest that 7-dehydrocholesterol (7-DHC)-derived oxysterols play important roles in the pathophysiology of Smith-Lemli-Opitz syndrome (SLOS), a metabolic disorder that is caused by defective 3 β -hydroxysterol- Δ^7 -reductase (DHCR7). Although 14 oxysterols have been identified as the primary products of 7-DHC autoxidation in organic solution, the metabolic fate of these oxysterols in a biological environment has not yet been elucidated. Therefore, we incubated these primary 7-DHC oxysterols in control Neuro2a and control human fibroblast cells and identified metabolites of these oxysterols by HPLC-MS. We also incubated *Dhcr7*-deficient Neuro2a cells and fibroblasts from SLOS patients with isotopically labeled 7-DHC (*d*₇-7-DHC). The observation of matching *d*₀- and *d*₇ peaks in HPLC-MS confirmed the presence of true metabolites of 7-DHC after excluding the possibility of ex vivo oxidation. The metabolites of primary 7-DHC oxysterols were found to contribute to the majority of the metabolic profile of 7-DHC in cells. Furthermore, based on this new data, we identified three new 7-DHC-derived metabolites in the brain of *Dhcr7*-KO mice. Our studies suggest that 7-DHC peroxidation is a major source of oxysterols observed in cells and in vivo and that the stable metabolites of primary 7-DHC oxysterols can be used as markers of 7-DHC peroxidation in these biological systems.—Xu, L., Z. Korade, D. A. Rosado, Jr., K. Mirnics, and N. A. Porter. Metabolism of oxysterols derived from nonenzymatic oxidation of 7-dehydrocholesterol in cells. *J. Lipid Res.* 2013. 54: 1135–1143.

Supplementary key words Smith-Lemli-Opitz syndrome • lipid peroxidation autoxidation • Neuro2a • fibroblast • mass spectrometry

7-Dehydrocholesterol (7-DHC) is the immediate biosynthetic precursor of cholesterol that accumulates in tissues and fluids of individuals affected with Smith-Lemli-Opitz syndrome (SLOS). SLOS is an autosomal recessive cholesterol biosynthesis disorder that is caused by mutations in the gene encoding 3 β -hydroxysterol- Δ^7 -reductase (DHCR7;

EC 1.3.1.21), the enzyme that catalyzes the reduction of 7-DHC to cholesterol. The defect in DHCR7 leads to an accumulation of 7-DHC and a pronounced reduction in the levels of cholesterol in affected individuals (1–7). SLOS is characterized by a broad spectrum of phenotypes, including multiple congenital malformations, neurological defects, brain abnormalities, mental retardation, autism-like behavior, and photosensitivity (6, 8–11).

We reported that 7-DHC is the most labile lipid molecule known to date toward free radical oxidation (autoxidation) (12). It is 200 times more reactive in autoxidation than cholesterol and more than 10 times more reactive than arachidonic acid (12). Over a dozen oxidation products (oxysterols) with novel structures were identified in the free radical oxidation of 7-DHC in solution (13, 14). We define these products as “primary nonenzymatically formed 7-DHC oxysterols” (or “primary 7-DHC oxysterols”) because they are formed outside of a biological environment and are thus not metabolized. More importantly, characteristic oxysterols were observed in cell and animal models for SLOS, such as *Dhcr7*-deficient Neuro2a cells, SLOS human fibroblasts, *Dhcr7*-KO mice, and AY9944-treated rats (14–16). However, the oxysterol profiles observed in these biological systems are distinctly different from the one observed in peroxidation of 7-DHC in solution, and major oxysterols formed from autoxidation in solution were not observed in cell and animal tissues (14–16).

Abbreviations: APCI, atmospheric pressure chemical ionization; BHT, butylated hydroxytoluene; Chol, cholesterol; 7-DHC, 7-dehydrocholesterol; DHCDO, 3 β ,5 α -dihydroxycholesta-7,9(11)-dien-6-one; DHCEO, 3 β ,5 α -dihydroxycholest-7-en-6-one; *Dhcr7* or DHCR7, 3 β -hydroxysterol- Δ^7 -reductase; 7-kChol, 7-ketocholesterol; 7-kDHC, 7-keto-cholesta-5,8-dien-3 β -ol; KO, knockout; NP, normal phase; 4 α -OH-7-DHC, 4 α -hydroxy-7-DHC; 4 β -OH-7-DHC, 4 β -hydroxy-7-DHC; 24-OH-7-DHC, 24-hydroxy-7-DHC; SLOS, Smith-Lemli-Opitz syndrome; SRM, selective reaction monitoring; THCEO, 3 β ,5 α ,9 α -trihydroxycholest-7-en-6-one; WT, wild-type.

¹To whom correspondence should be addressed.
e-mail: libin.xu@vanderbilt.edu (L.X.); n.porter@vanderbilt.edu (N.A.P.)

²Present address of D. A. Rosado, Jr.: Department of Chemistry & Biochemistry, Mississippi College, Clinton, MS 39058.

^SThe online version of this article (available at <http://www.jlr.org>) contains supplementary data in the form of two figures.

This work was supported by National Institutes of Health Grants ES-013125 (N.A.P.), HD-064727 (N.A.P.), K99-HD-073270 (L.X.), and MH-079299 (K.M.).

Manuscript received 8 January 2013 and in revised form 27 January 2013.

Published, JLR Papers in Press, February 1, 2013

DOI 10.1194/jlr.M035733

Oxysterols as a class can exert a broad spectrum of biological functions in cells and tissues. Among the functions affected are cell apoptosis, activation of the inflammatory response, regulating cholesterol homeostasis and hedgehog signaling pathways, and modulating immune system responses (17–19). Individual oxysterols formed from free radical oxidation of 7-DHC exert differential cytotoxicity to cells, and the oxysterol mixture leads to changes in cell proliferation, differentiation, and gene expression (20). One of the major 7-DHC-derived oxysterols observed in cell and animal models of SLOS, 3 β ,5 α -dihydroxycholest-7-en-6-one (DHCEO), induces critical gene expression changes that relate to cell growth and lipid biosynthesis (14, 20). This compound also accelerates differentiation and arborization of cortical neurons (21). Mechanistic studies in Neuro2a cells suggested that DHCEO is formed from one of the primary oxysterols of 7-DHC peroxidation, 7-DHC-5 α ,6 α -epoxide, via the intermediate 7-cholesten-3 β ,5 α ,6 β -triol (14). However, the mechanisms of formation of other endogenous oxysterols, as well as the metabolic fate of other primary 7-DHC oxysterols, are still unknown.

We have investigated the metabolism of 7-DHC and its oxysterols in cell cultures and we report the following here: *i*) the elucidation of the metabolic profile of 7-DHC in *Dhcr7*-deficient Neuro2a cells and SLOS human fibroblasts by incubating deuterium-labeled 7-DHC (*d*₇-7-DHC) in these cell lines followed by HPLC-MS analysis; *ii*) identification of the metabolites of primary oxysterols of 7-DHC autoxidation in control Neuro2a cells and control human fibroblasts by HPLC-MS; *iii*) correlation of the metabolites of the primary 7-DHC oxysterols to the overall metabolic profiles of 7-DHC in *Dhcr7*-deficient Neuro2a cells and SLOS human fibroblasts; and *iv*) identification of three new 7-DHC-derived oxysterols in brain of *Dhcr7*-KO mice based on the metabolic profile of primary 7-DHC oxysterols.

MATERIALS AND METHODS

Materials

HPLC-grade solvents (hexanes and 2-propanol) were purchased from Thermo Fisher Scientific Inc. [25,26,26,26,27,27,27-*d*₇]-7-DHC, *d*₇-DHCEO, 4 α -hydroxy-7-DHC, 4 β -hydroxy-7-DHC, and cholesta-7-en-3 β ,5 α ,6 α (β),9 α -tetraols were prepared as reported previously (14, 15). Other standards of 7-DHC-derived oxysterols, including compounds **1**, **2a**, **2b**, **3**, **4**, **5**, **6a**, **6b**, 3 β ,5 α ,9 α -trihydroxycholest-7-en-6-one (THCEO), and 3 β ,5 α -dihydroxycholesta-7,9(11)-dien-6-one (DHCEO) were isolated from the product mixture of free radical oxidation of 7-DHC in solution (13). 7-Keto-cholesta-5,8-dien-3 β -ol (7-kDHC) was synthesized as described below. All other chemical reagents at the highest grade were purchased from Sigma-Aldrich Co. and were used without further purification. NH₂-SPE cartridges (55 μ m, 70 Å, 500 mg/3 ml) were purchased from Phenomenex Inc.

Cell cultures and treatment of human fibroblasts and Neuro2a cells

Neuroblastoma cell line Neuro2a was purchased from the American Type Culture Collection (Rockville, MD). Control (GM05399 and GM05565) and SLOS (GM05788 and GM03044)

human fibroblasts (HF) were purchased from the Coriell Institute. *Dhcr7*-deficient Neuro2a cells were generated as described previously (22). All cell lines were maintained in DMEM supplemented with L-glutamine, 10% fetal bovine serum (FBS; Thermo Scientific HyClone, Logan, UT), and penicillin/streptomycin at 37°C and 5% CO₂. Generally for different treatment, the HF cells were plated at a density of 3.0 \times 10⁵ cells/plate in 60 mm cell culture dishes (Sarstedt, Newton, NC), whereas the Neuro2a cells were plated at a density of \sim 1 \times 10⁶ cells/plate in 100 mm dishes. Both cell lines were allowed 12 h to attach to the dishes. For treatment of *Dhcr7*-deficient Neuro2a cells or SLOS HFs, cells were cultured in the presence of different concentrations of *d*₇-7-DHC in DMEM medium containing 10% lipid-reduced serum (HyClone Lipid Reduced FBS, Thermo Fisher Scientific Inc.), L-glutamine, and penicillin/streptomycin for five days (medium was refreshed every two days). This lipid-reduced FBS does not contain a detectable level of cholesterol.

When treating control Neuro2a cells or control HF cells with different primary 7-DHC-derived oxysterols, the cells were cultured in the presence of different oxysterols (1 μ M for compounds **2a**, **2b**, and **3**, and 5 μ M for other oxysterols due to their different toxicity) (20) in medium with 10% regular FBS. At the end of the experiments, the cells were washed with 1 \times PBS buffer twice, scraped with a cell scraper, and centrifuged at 250 *g* for 5 min at 4°C. The cell pellets were frozen at –80°C until lipid extraction and separation.

Dhcr7-KO mice

Dhcr7-KO (*Dhcr7*^{m1Gst/J}) mice were purchased from Jackson Laboratories (catalog #007453). The mice were kept and bred in Division of Animal Care facilities at Vanderbilt University. All experimental procedures were in accordance with the National Institutes of Health guidelines for the use of live animals and were approved by the Vanderbilt University Institutional Animal Care and Use Committee. Genotyping and dissection of the tissues from P0 or E20 mice were performed as previously described (14). The brain tissues were rapidly removed and frozen in pre-cooled methyl-butane and stored at –80°C until lipid extraction and HPLC-APCI-MS/MS analysis.

Lipid extraction, separation, and HPLC-APCI-MS/MS analyses

Extraction and separation of the lipids from cell pellets and brain tissues were described in detail previously (14). The cells treated with *d*₇-7-DHC were processed in the absence of any deuterated oxysterol standard, and the cells treated with 7-DHC-derived oxysterols were processed in the presence of an appropriate amount of *d*₇-DHCEO standard. Briefly, to the cell pellets was added Folch solution [5 ml chloroform/methanol (2/1) containing 0.001M BHT and PPh₃], followed by the addition of NaCl aqueous solution (0.9%, 1 ml). The resulting mixture was vortexed for 1 min and centrifuged for 5 min. The lower organic phase was recovered, dried under a stream of nitrogen, redissolved in methylene chloride, and subjected to separation with NH₂-SPE [500 mg cartridge; the column was conditioned with 4 ml of hexanes, and the neutral lipids containing oxysterols were eluted with 4 ml of chloroform/2-propanol (2/1)]. The eluted fractions were then dried under nitrogen and reconstituted in methylene chloride (200 μ l) for normal phase (NP) HPLC-APCI-MS/MS analyses following a previously reported method (13, 20). HPLC was performed with either a 5 μ m 250 \times 4.6 mm silica column (Beckman Coulter Inc.) or a 3 μ m 150 \times 4.6 mm silica column (Phenomenex Inc.). A gradient of 2-propanol in hexanes was used as the elution solvent at 1.0 ml/min: 2-propanol/hexanes = 10/90 (0–15 min), 19/81 (16–26 min), 10/90 (27–35 min). MS analysis was performed on a ThermoFinnigan TSQ Quantum Ultra

coupled to the HPLC. Selective reaction monitoring (SRM) was employed to monitor the dehydration process of the ion $[M+H]^+$ (to $[M+H-H_2O]^+$) or $[M+H-H_2O]^+$ (to $[M+H-2H_2O]^+$) in the mass spectrometry (14, 15).

Synthesis of 7-kDHC

7-Hydroperoxy-cholesta-5,8-dien-3 β -ol (7-kDHC; 37 mg prepared as described in Ref. 23) was stirred in pyridine (1 ml) and acetic anhydride (1 ml) at room temperature overnight, followed by the removal of pyridine under vacuum. The resulting mixture was then diluted with ethyl acetate (10 ml), washed with saturated aqueous sodium bicarbonate (10 ml \times 2) and 5% hydrochloric acid (10 ml), dried over magnesium sulfate, filtered, and evaporated to give a crude product of 7-kDHC acetate. The crude 7-kDHC acetate was then redissolved in ethanol (3 ml), to which sodium methoxide (20 mg) was added. The reaction was stirred at room temperature for 30 min and was diluted with saturated aqueous ammonium chloride. The resulting mixture was extracted with methylene chloride (10 ml \times 3), dried over magnesium sulfate, filtered, and evaporated to give crude 7-kDHC. Flash column chromatography on silica gel (elution solvent: hexanes/ethyl acetate = 1/1) gave pure 7-kDHC as an amorphous white solid (20 mg, 56% of yield over two steps). 1H NMR (600 MHz, $CDCl_3$): δ 0.63 (s, 3H), 0.86 (d, 3H, $J=3.0$ Hz), 0.87 (d, 3H, $J=3.0$ Hz), 0.95 (d, 3H, $J=6.6$ Hz), 1.36 (s, 3H), 1.66–1.76 (m, 1H), 1.93–2.02 (m, 2H), 2.04–2.12 (m, 2H), 2.20–2.27 (m, 2H), 2.35–2.42 (m, 1H), 2.43–2.50 (m, 1H), 2.53 (dt, 1H, $J=11.9, 1.2$ Hz), 2.55–2.62 (m, 2H), 3.65 (m, 1H), 6.03 (d, 1H, $J=1.1$ Hz). ^{13}C NMR (150 MHz, $CDCl_3$): δ 11.8, 19.0, 22.7, 22.9, 23.8, 24.0, 24.76, 24.83, 28.1, 29.5, 30.7, 34.8, 35.8, 36.2, 36.3, 39.6, 42.0, 42.1, 42.6, 48.5, 53.6, 72.0, 126.8, 134.1, 161.5, 162.0, 186.6.

RESULTS

Oxysterol metabolic profile of 7-DHC in *Dhcr7*-deficient Neuro2a cells

We reported previously that a number of HPLC-MS fractions that have molecular mass corresponding to oxysterols have been found in the analysis of lipid from *Dhcr7*-deficient Neuro2a cells and SLOS human fibroblasts, when the analysis was compared with matching control samples. However, only one of these new peaks, DHCEO, has been identified (14). To identify the additional unknown peaks, we incubated these two cell lines in medium containing lipid-reduced serum supplemented with d_7 -7-DHC, and we analyzed the oxysterols in the cells by HPLC-MS (see Materials and Methods).

A typical HPLC-MS chromatogram of *Dhcr7*-deficient Neuro2a cells treated with d_7 -7-DHC is shown in Fig. 1A. Mass-to-charge ratios that correspond to both d_0 -oxysterols and corresponding d_7 -oxysterols were monitored. As seen in Fig. 1, several new peaks were observed in the matching d_0 and d_7 panels, suggesting that these products are potential metabolites of 7-DHC. No 7-DHC-derived peak was observed after 11 min of the chromatogram. The peaks were identified as 4 α -hydroxy-7-DHC, 4 β -hydroxy-7-DHC, 7-keto-cholesta-5,8-dien-3 β -ol (7-kDHC), 3 β ,5 α ,9 α -trihydroxycholest-7-en-6-one (THCEO), and 3 β ,5 α -dihydroxycholesta-7,9(11)-dien-6-one (DHCDO) by comparing the retention time (RT) and MS characteristics

with synthetic standards of these compounds (13, 15). The structures of these oxysterols are shown in Fig. 2. Furthermore, two unknown 7-DHC-derived peaks were observed in the m/z panels that correspond to $[7\text{-DHC}+10+H]^+$ and $[7\text{-DHC}+10+H^+-H_2O]$ (unknown-1 and unknown-2).

Because 7-DHC is exceptionally oxidizable, we sought to exclude the possibility that the observed oxysterols were formed during sample collection and preparation. We processed control samples of *Dhcr7*-deficient Neuro2a cells (grown in the absence of d_7 -7-DHC) in the presence of externally added d_7 -7-DHC and compared the ratios of the d_7 - and corresponding d_0 -oxysterols to the ratio of d_7 - and d_0 -7-DHC in the cells (Fig. 3). If the ratio of d_7/d_0 determined for a given oxysterol was significantly less than the measured d_7/d_0 -7-DHC ratio, the oxysterol was likely formed in the live cell. If the d_7/d_0 ratio of an oxysterol is comparable to the d_7/d_0 ratio of its 7-DHC precursor, then this oxysterol was formed during sample processing. From this experiment, we confirmed that all 4 α -hydroxy-7-DHC, 4 β -hydroxy-7-DHC, and unknown-2; a majority of DHCEO, THCEO, DHCDO, and 7-kDHC; and \sim 50% of unknown-1 are formed in cells, suggesting that these oxysterols are indeed metabolites of 7-DHC in cells.

Oxysterol metabolic profile of 7-DHC in SLOS human fibroblasts

The metabolic profile of 7-DHC in SLOS human fibroblasts is similar to the one observed for *Dhcr7*-deficient Neuro2a cells, but with DHCEO being the major metabolite present (Fig. 1B). Specifically, 4 α -hydroxy- and 4 β -hydroxy-7-DHC were only observed as very minor metabolites in fibroblasts and the unknown peak (unknown-2) in the m/z panel of $[7\text{-DHC}+10+H]^+$ was not observed.

Although the metabolic profile is similar between *Dhcr7*-deficient Neuro2a cells and SLOS human fibroblasts, there are clear differences in the way metabolites are formed, as indicated by the d_7/d_0 ratio of each metabolite. In human fibroblasts, every metabolite has a larger d_7/d_0 ratio than the d_7/d_0 ratio of 7-DHC (Fig. 4A). This is not surprising since d_7 -7-DHC is present at the beginning of the cell treatment (allowing d_7 -oxysterol formation at an earlier stage), but d_0 -7-DHC accumulates slowly by biosynthesis over the course of incubation in lipid-reduced medium. However, in *Dhcr7*-deficient Neuro2a cells, only the d_7/d_0 ratios of DHCEO, 7-kDHC, THCEO, DHCDO, and unknown-1 were larger than that of 7-DHC. The d_7/d_0 ratios of 4 α -hydroxy-7-DHC, 4 β -hydroxy-7-DHC and unknown-2 were not different from the same ratio of 7-DHC (Fig. 4B).

Another metabolic difference between these two cell lines is that d_7 -7-DHC was converted to d_7 -cholesterol to different extents. The d_7/d_0 ratio of cholesterol is comparable to that of 7-DHC in *Dhcr7*-deficient Neuro2a cells (0.033 versus 0.038), but is only ca. 6% of the same ratio of 7-DHC in SLOS human fibroblasts (0.011 versus 0.18). This difference is presumably due to the fact that the *Dhcr7*-deficient (knockdown by shRNA) Neuro2a cells still retain some activities of *Dhcr7* (22).

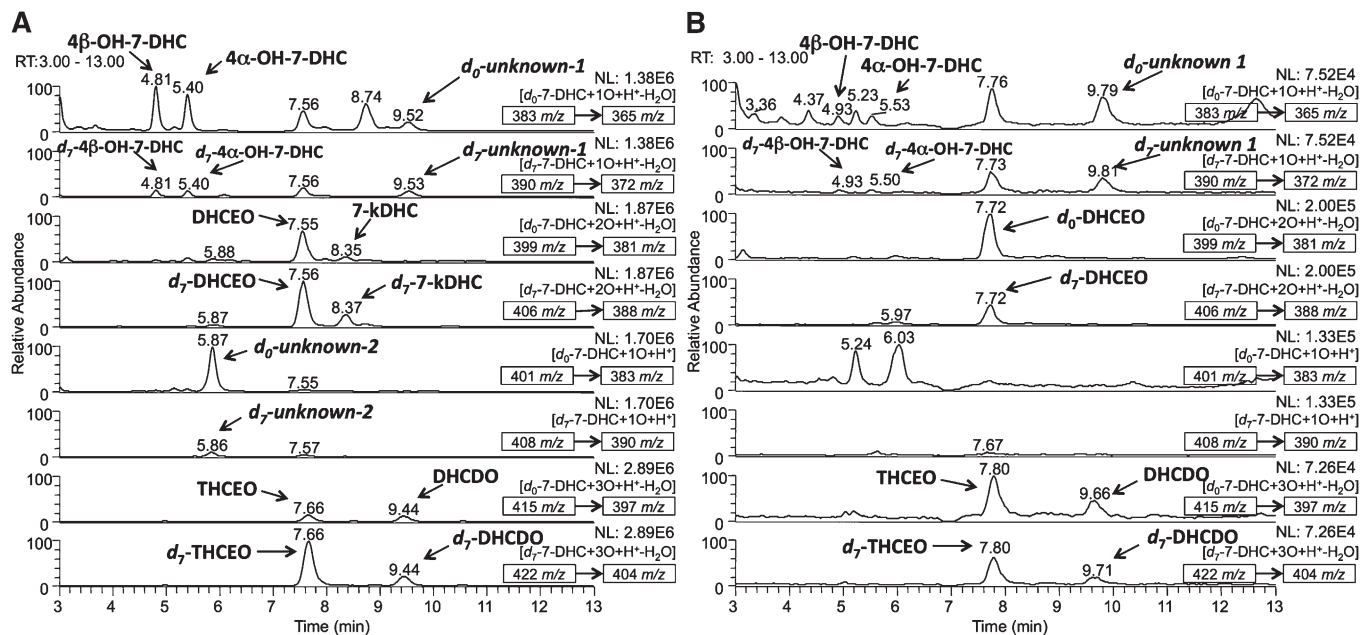


Fig. 1. NP-HPLC-APCI-MS/MS (silica 4.6 mm \times 150 mm column; 3 μ m; 1.0 ml/min; elution solvent: 10% 2-propanol in hexanes) analysis of the oxysterols from (A) *Dhc7*-deficient Neuro2a cells that were incubated in the presence of 5 μ M of *d*₇-7-DHC in lipid-reduced medium for five days and (B) SLOS human fibroblasts incubated in the presence of 1 μ M of *d*₇-7-DHC in the same manner. Peaks that were observed in both the *d*₀-oxysterol and the *d*₇-oxysterol MS panels at the same retention time were identified as metabolites of 7-DHC. No 7-DHC-derived peak was observed after 13 min (not shown). The parent ion of each chromatogram and the MS/MS transition are marked in the corresponding MS panel.

Oxysterol metabolic profile of primary nonenzymatically formed 7-DHC-derived oxysterols in control Neuro2a cells and control human fibroblasts

We presume that primary nonenzymatically formed 7-DHC oxysterols are further metabolized to more stable oxysterols in cells and tissues. To examine this hypothesis, we incubated major primary 7-DHC autooxidation-derived oxysterols and cholesta-7-en-3 β ,5 α ,6 α (β),9 α -tetraols [6 α (β)-tetraols] (**Fig. 5**) in control Neuro2a cells and control human fibroblasts, and we analyzed the metabolites of these oxysterols by HPLC-MS. Noncytotoxic concentrations of oxysterols (1 μ M for compounds **2a** and **2b**, and 5 μ M for other compounds) were used in this study based on our previous study in Neuro2a cells (20). At these concentrations, the oxysterols did not induce changes in the cell viability and morphology of these two cell lines. The same amount of *d*₇-DHCEO was added to each sample during

processing for comparison between relative peak intensity and retention time. No 7-DHC-derived oxysterol was observed in vehicle-treated control cells (**Fig. 6A** and supplementary Fig. IIA). From the HPLC-MS analysis shown in Fig. 6 and supplementary Figs. I and II, we found that the main metabolic pathways that operate are reduction of endoperoxide, epoxide ring opening, and oxidation of allylic alcohol (**Fig. 7**). For example, compound **1** was apparently metabolized to the 6 β -tetraol by epoxide ring opening, an intermediate that was further metabolized to THCEO via oxidation of the allylic alcohol to ketone (Fig. 6B). Compounds **2a** and **2b** were metabolized to 6 α -tetraol and 6 β -tetraol via the reduction of the endoperoxide, respectively, followed by conversion to THCEO via allylic oxidation (Fig. 6C, D). Although metabolites of compound **3** were not identified due to lack of standards, this oxysterol presumably undergoes endoperoxide reduction, epoxide

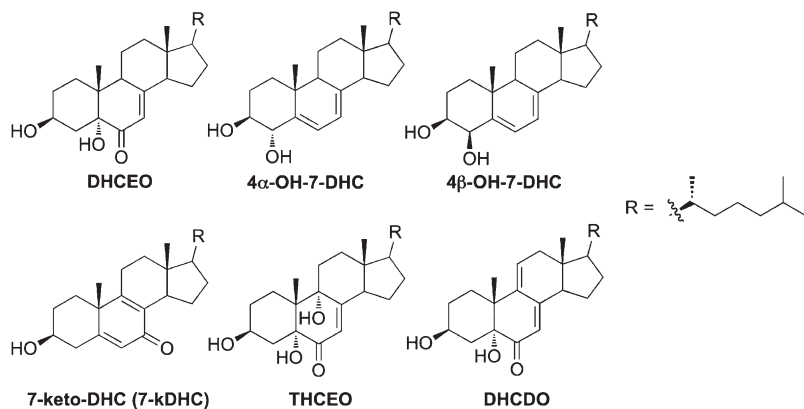


Fig. 2. Structures of identified 7-DHC-derived oxysterols in *Dhc7*-deficient Neuro2a cells and/or SLOS human fibroblasts.

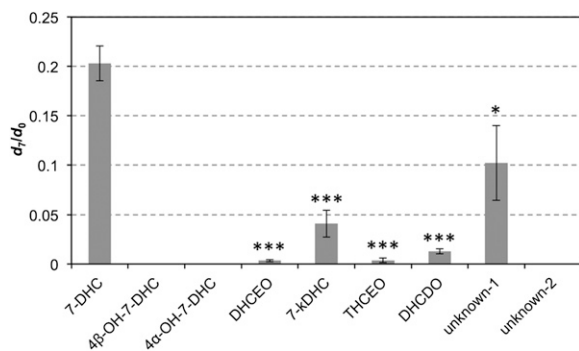


Fig. 3. Evaluation of oxysterol formation during sample processing of *Dhcr7*-deficient Neuro2a. Cell samples were cultured in the absence of d_7 -7-DHC but processed in the presence of externally added d_7 -7-DHC. The ratio of d_7/d_0 -oxysterol is compared with the same ratio of 7-DHC. All ratios of d_7/d_0 -oxysterols were found to be significantly less than the ratio of d_7/d_0 -7-DHC. Statistical analyses were performed with *t*-test (two-tailed distribution) against d_7/d_0 ratio of 7-DHC. N = 3; * P < 0.05; *** P < 0.0005.

ring opening, and/or dehydration (supplementary Fig. I). The structures of these metabolites are proposed based on the MS characteristics and the retention time (polarity) of each metabolite as shown in supplementary Fig. I. The metabolites of compound **4** were not clearly detected in Neuro2a cells, but triene **5** was formed from compound **4** in control human fibroblasts (supplementary Fig. II).

There are some differences in the reactivities of different oxysterols for the similar metabolic transformations. For example, the 6 α - and 6 β -tetraols both contain an allylic

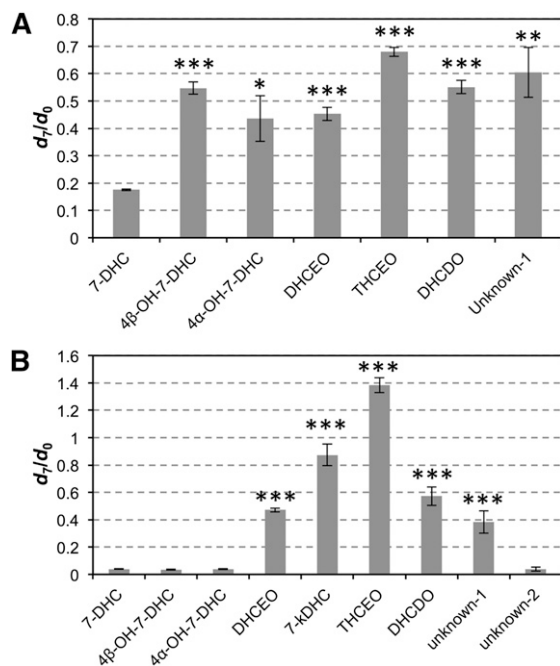


Fig. 4. Comparison of d_7/d_0 ratios of 7-DHC-derived metabolites to the d_7/d_0 ratio of 7-DHC in (A) SLOS human fibroblasts and (B) *Dhcr7*-deficient Neuro2a cells that were incubated in the presence of 1 μ M of d_7 -7-DHC in lipid-reduced medium for five days. Statistical analyses were performed with *t*-test (two-tailed distribution) against d_7/d_0 ratio of 7-DHC. N = 3; * P < 0.05; ** P < 0.005; *** P < 0.0005.

alcohol, but the 6 β -tetraol is clearly more prone to allylic oxidation as indicated by the formation of much higher level of THCEO from this substrate than from the 6 α compound under the same conditions (Fig. 6E, F). In addition, the allylic alcohol at C6 having a double bond at C7 = C8 appears to be much more reactive toward oxidation than the one at C7 with the double bond at C8 = C14 (from metabolism of compounds **6a** and **6b**) as no ketone products were observed as metabolites of compounds **6a** and **6b** (no peak with a m/z value of the potential ketone product was observed) (supplementary Fig. II).

Identification of THCEO, DHCDO, and 7-kDHC in brain of *Dhcr7*-KO mice

To establish whether the oxysterol profile in the nervous system reflects the profile identified in the neuronal cell line, we examined the oxysterols formed in brain of *Dhcr7*-KO mice at P0 (E20). Although we have previously identified several oxysterols in brain of the KO mice, [including 24-hydroxy-7-DHC, DHCEO, 4 α -hydroxy-7-DHC, and 4 β -hydroxy-7-DHC (16)], several oxysterols remained unidentified. With the knowledge obtained from our studies of oxysterol metabolism in cells, we found three previously unidentified oxysterols, THCEO, DHCDO, and 7-kDHC, based on the retention time and MS characteristics by comparing with the standards of these oxysterols and d_7 -DHCEO (Fig. 8B). A few minor peaks remain unidentified due to lack of matching standards. No 7-DHC-derived oxysterol was observed in brain of wild-type mice (Fig. 8A). At E20 or P0, the identified oxysterols reflect primarily neuronal metabolism because glial cell development and myelination proceed postnatally (24, 25). Therefore, the presence of these identified oxysterols suggests that 7-DHC peroxidation in neurons proceeds in a way similar to that in the Neuro2a cell line. Future studies in hypomorphic mouse models will allow us to compare glial and neuronal metabolism of 7-DHC-derived oxysterols (26).

DISCUSSION

Free radical oxidation of 7-DHC in solution gives over a dozen oxysterols as products, and these oxysterols are found to exert a variety of biological activities, including cytotoxicity and induction of gene expression changes (13, 20, 21). However, the oxysterol profiles found in cell and rodent models of SLOS are distinctly different from the peroxidation product profile observed from authentic free radical oxidation in organic solvent. Our studies here suggest that the primary oxysterols formed from 7-DHC peroxidation are further metabolized in biological environments, leading to the observed differences in the oxysterol profiles.

The studies reported here clearly establish links between the primary oxysterols derived from 7-DHC autoxidation and the oxysterol metabolites observed in cell and animal SLOS models. The incubation experiments in *Dhcr7*-deficient Neuro2a cells and SLOS human fibroblasts with d_7 -7-DHC (Fig. 1) and the ex vivo oxidation tests (Fig. 3)

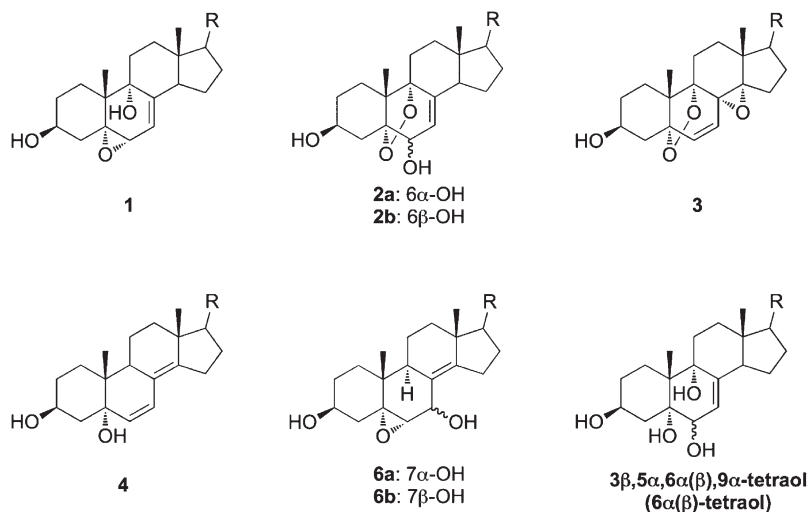


Fig. 5. Structures of primary 7-DHC peroxidation-derived oxysterols and cholesta-7-en-3 β ,5 α ,6 α (β),9 α -tetraol that were incubated in control Neuro2a and human fibroblast cells for metabolism studies.

unequivocally identified the metabolites that are derived from 7-DHC in cell culture. The identified products include 4 α -hydroxy-7-DHC, 4 β -hydroxy-7-DHC, 7-kDHC, DHCEO, THCEO, and DHCDO (Fig. 2). 4 α -Hydroxy-7-DHC and 4 β -hydroxy-7-DHC have been identified in tissues

of rodent models of SLOS (15, 16), and they are likely formed from enzymatic oxidation of 7-DHC as they were not isolated as products of free radical oxidation of 7-DHC in solution (13). However, the origin of these two oxysterols is still debatable as 4 β -hydroxycholesterol, but not

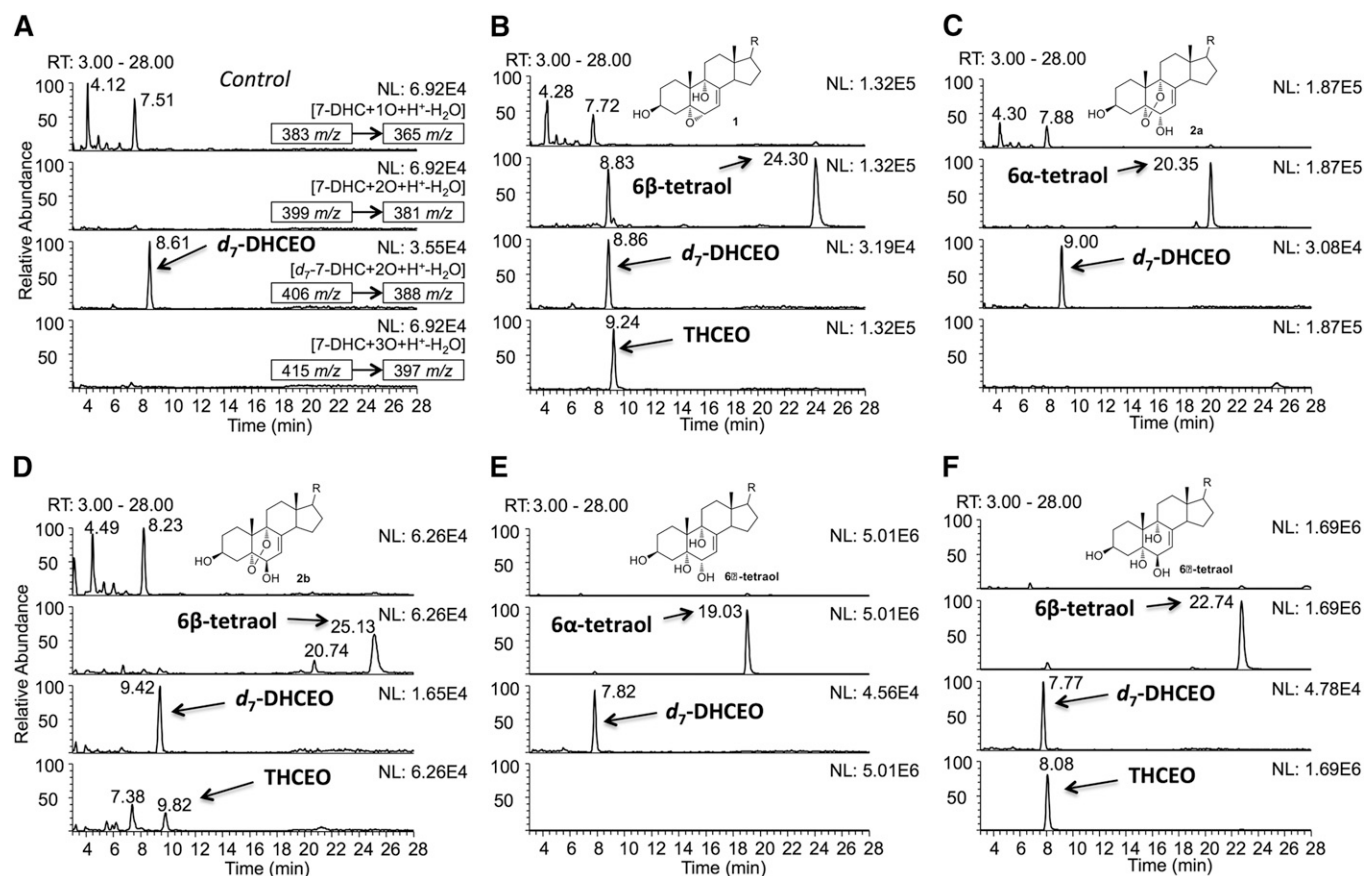


Fig. 6. NP-HPLC-APCI-MS/MS [silica 4.6 mm × 250 mm column; 5 μ m; 1.0 ml/min; elution solvent: 2-propanol/hexanes = 10/90 (0–15 min), 19/81 (16–26 min), 10/90 (27–35 min)] analysis of the oxysterols in (A) control Neuro2a cells and Neuro2a cells that were incubated in the presence of (B) 5 μ M of **1**, (C) 1 μ M of **2a**, (D) 1 μ M of **2b**, (E) 5 μ M of 6 α -tetraol, and (F) 5 μ M of 6 β -tetraol for 24 h in DMEM medium that was supplemented with regular FBS. The structures of the oxysterols incubated in each experiment are shown in the corresponding chromatogram. A known amount of *d*₇-DHCEO was added to each sample as an internal standard so that retention time and peak intensities of the peaks could be compared between each run. The parent ion and the MS/MS transition are marked in each panel of (A), and the same MS/MS transitions were monitored in every experiment.

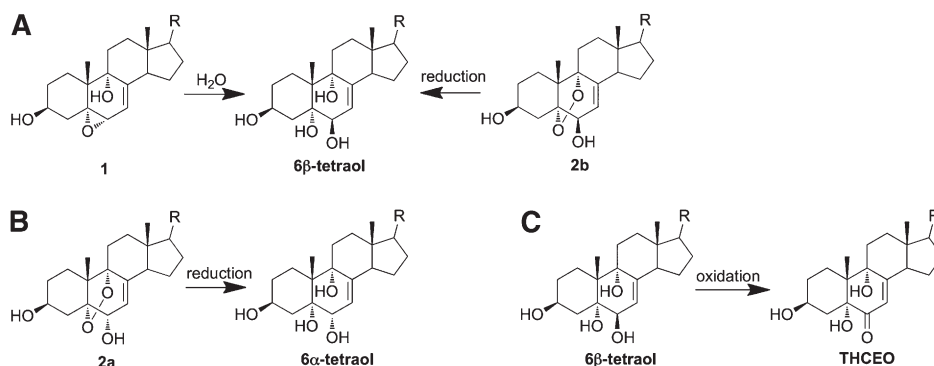


Fig. 7. Major metabolic pathways of primary 7-DHC-derived oxysterols: reduction of endoperoxide (A, B), epoxide ring opening (A), and oxidation of allylic alcohol (C).

4 α -hydroxycholesterol, was identified as an enzymatic oxidation product of cholesterol via the catalysis of CYP 3A4 (27, 28). More importantly, DHCEO and THCEO are also identified as the stable end metabolic products of primary oxysterols of 7-DHC peroxidation, suggesting that peroxidation of 7-DHC contributes significantly to the overall oxysterol pool in cell culture and in vivo (Figs. 1 and 6). We note that DHCEO and THCEO are very minor products of 7-DHC autoxidation, yet they are among the major metabolites observed in cells and in vivo. This is perhaps not surprising since their precursors, 7-DHC-5 α ,6 α -epoxide and compounds **1**, **2a**, and **2b**, are major primary oxysterols formed from 7-DHC autoxidation (13).

The primary oxysterols formed from 7-DHC autoxidation in solution are biologically active in control Neuro2a cells and in cortical neuronal cells, being cytotoxic and inducing changes in gene expression and morphology (20, 21). In Neuro2a cells, a mixture of the primary 7-DHC oxysterols downregulates gene transcripts related to lipid biosynthesis (including *Hmgcr*, *Dhcr7*, *Srebp2*, *Fasn*, *S1p*, and *Sqs*) and cell growth (including *Ki67*, *Adam19*, and *Egr1*) (20). While the stable metabolites of the primary oxysterols can be used as biomarkers of 7-DHC peroxidation, they may by themselves exert various biological activities. For example, DHCEO is not only toxic to neuronal cells but also induces changes in critical gene transcripts (20). Accelerated

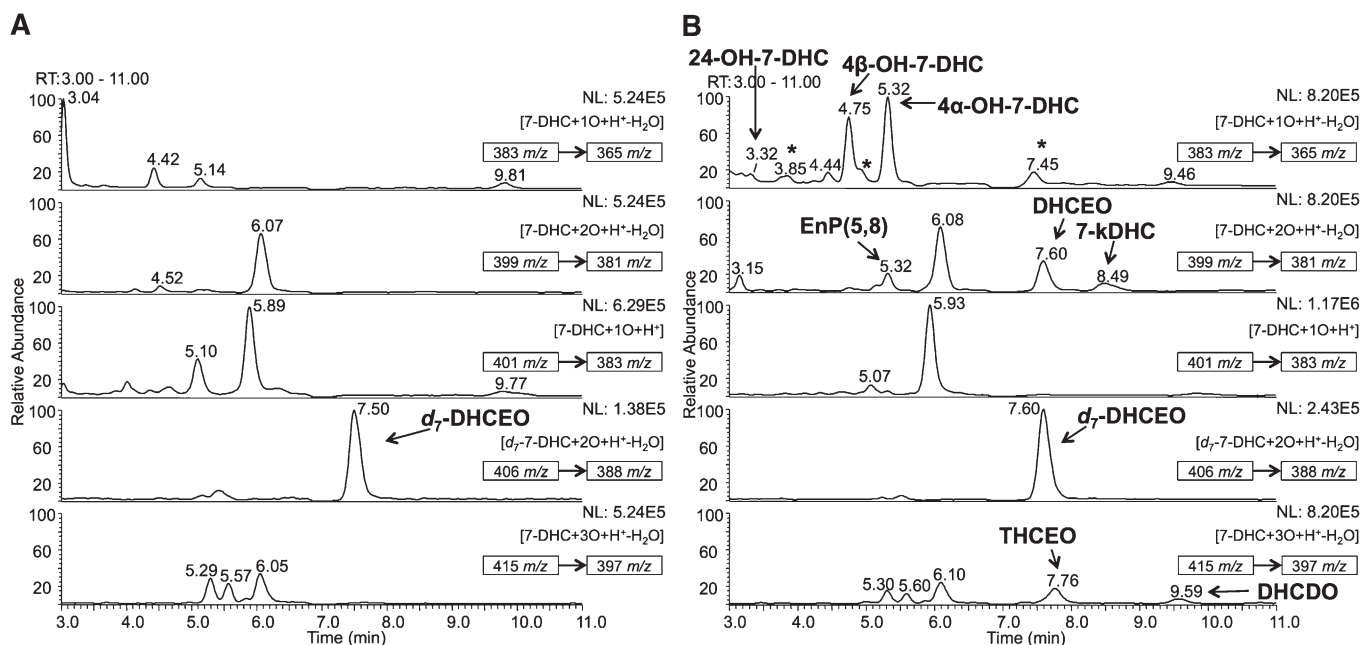


Fig. 8. NP-HPLC-APCI-MS/MS (silica 150 \times 4.6 mm column; 3 μ ; 1.0 ml/min; elution solvent: 10% 2-propanol in hexanes) analysis of the oxysterols from (A) WT and (B) *Dhcr7*-KO mouse brains at P0 or E20. In (B), DHCEO, 4 α -hydroxy-7-DHC, 4 β -hydroxy-7-DHC, and 24-hydroxy-7-DHC were identified previously (15, 16), while THCEO, DHCEO, and 7-kDHC were identified in this study. A known amount of *d*₇-DHCEO was added to each sample as an internal standard so that retention time and peak intensities of the peaks could be compared between each run. New and unidentified peaks observed in KO mice relative to WT are marked with an asterisk. 5 α ,8 α -Epidioxycholest-6-en-3 β -ol (EnP) (5, 8) is a photooxidation product of 7-DHC that has been demonstrated to be a product of ex vivo oxidation (15). The parent ion of each chromatogram and the MS/MS transition are marked in the corresponding MS panel.

cell differentiation has also been observed in both Neuro2a cells and primary neurons treated with DHCEO (20, 21).


The main metabolic pathways from the primary 7-DHC autoxidation products to the stable oxysterols observed in cells appear to be the reduction of endoperoxides, epoxide ring opening, and oxidation of allylic alcohols (Fig. 7). These transformations can be understood based on the reducing biological environment of cells, the presence of cellular epoxide hydrolases, and the high reactivity of allylic alcohols. As an example, cholesterol 5,6-epoxide (α or β) can be readily converted to cholesta-3 β ,5 α ,6 β -triol by Δ^5 -steroid epoxide hydrolase (29–31), and evidence also supports its subsequent oxidation to 3 β ,5 α -dihydroxycholestan-6-one (31, 32). In addition, both 7 α - and 7 β -hydroxycholesterol can be oxidized via allylic oxidation through the catalysis of 7 α -hydroxysterol dehydrogenase to give 7-ketocholesterol, an analog of 7-kDHC (33).

7-KDHC is a novel 7-DHC-derived oxysterol that is presumably formed from dehydration of 7-hydroperoxycholesta-5,8-dien-3 β -ol. 7-Hydroperoxycholesta-5,8-dien-3 β -ol is a known product of 7-DHC photo-oxidation (23), but it can also be formed from free radical oxidation of 7-DHC when good hydrogen atom donors, such as vitamin E, are present in the reaction (13, 34).

The observed d_7/d_0 ratios of the oxysterols shed light on the differences in metabolism between the two different cell lines studied. As seen in Fig. 4, the d_7/d_0 ratios of all oxysterols in human fibroblasts are larger than the d_7/d_0 ratio of the precursor 7-DHC, which is reasonable considering d_7 -7-DHC is present at high concentrations even during the early stages of treatment. In addition, the d_7/d_0 ratios are quite similar among all oxysterols, suggesting that d_7 -7-DHC is essentially equivalent to d_0 -7-DHC during its metabolism in human fibroblasts. In Neuro2a cells, most of the d_7/d_0 -oxysterol ratios are larger than the 7-DHC ratios, but 4 α -hydroxy-7-DHC, 4 β -hydroxy-7-DHC, and unknown-2 have ratios comparable to that of 7-DHC (Fig. 4B), suggesting that exogenously added d_7 -7-DHC and metabolically derived d_0 -7-DHC are differentiated by some of the subsequent metabolic pathways. Thus, it is reasonable to speculate that the differences in oxysterol profiles between these two cell lines may be due to *i*) their different metabolic activities, as Neuro2a is an immortal neuroblastoma cell line and human fibroblast is a primary cell line; *ii*) their different expression of enzymes responsible for the metabolic transformations; *iii*) their different antioxidant capacity; and *iv*) different access of endogenous d_0 - and exogenous d_7 -7-DHC to the necessary enzymes. For example, it is known that cholesterol is mainly synthesized in endoplasmic reticulum in cells (35), whereas the exogenously added d_7 -7-DHC presumably resides mostly in the membrane.

The metabolites of the primary nonenzymatically formed 7-DHC oxysterols are also observed in the brain of *Dhcr7*-KO mice. In addition to the known DHCEO (14–16), we identified THCEO, DHCDO, and 7-kDHC in this study. Note that the oxysterol profiles between *Dhcr7*-deficient Neuro2a cells and the *Dhcr7*-KO brain are quite similar, suggesting that Neuro2a cells are a good model to study

the metabolism of primary 7-DHC oxysterols, at least for the rodent models of SLOS. Our metabolism studies in cells reasonably explain the distinct differences between the oxysterol profiles in solution and in vivo. The observation of these stable metabolites of the primary peroxidation products of 7-DHC establishes that the origin of a large proportion of the 7-DHC-derived oxysterols in brain of *Dhcr7*-KO mice is via peroxidation, which fortifies the link between 7-DHC peroxidation and the pathophysiology of SLOS.

Identification of stable metabolites of 7-DHC in specific cell types and tissues allows future research on their biological activities and their contribution to SLOS pathophysiology. As these 7-DHC-derived oxysterols are almost universally observed in vitro and in vivo (14–16, 20, 21, 36), the findings reported here on metabolic mechanisms pave the way for the development and testing of new approaches to reduce the levels of these oxysterols in vivo. Indeed, we have previously demonstrated that antioxidant supplementation reduced the levels of DHCEO in SLOS human fibroblasts (14). Thus, the combination of all 7-DHC-derived oxysterol biomarkers may provide a critical tool in diagnosis, disease progression monitoring, therapy development, and treatment efficacy monitoring. 

Z.K. appreciates support from the Vanderbilt Kennedy Center for Research on Human Development.

REFERENCES

1. Irons, M., E. R. Elias, G. Salen, G. S. Tint, and A. K. Batta. 1993. Defective cholesterol biosynthesis in Smith-Lemli-Opitz syndrome. *Lancet*. **341**: 1414.
2. Tint, G. S., M. Irons, E. R. Elias, A. K. Batta, R. Frieden, T. S. Chen, and G. Salen. 1994. Defective cholesterol biosynthesis associated with the Smith-Lemli-Opitz syndrome. *N. Engl. J. Med.* **330**: 107–113.
3. Fitzky, B. U., F. F. Moebius, H. Asaoka, H. Waage-Baudet, L. Xu, G. Xu, N. Maeda, K. Kluckman, S. Hiller, H. Yu, et al. 2001. 7-Dehydrocholesterol-dependent proteolysis of HMG-CoA reductase suppresses sterol biosynthesis in a mouse model of Smith-Lemli-Opitz/RSH syndrome. *J. Clin. Invest.* **108**: 905–915.
4. Krakowiak, P. A., N. A. Nwokoro, C. A. Wassif, K. P. Battaile, M. J. Nowaczyk, W. E. Connor, C. Maslen, R. D. Steiner, and F. D. Porter. 2000. Mutation analysis and description of sixteen RSH/Smith-Lemli-Opitz syndrome patients: polymerase chain reaction-based assays to simplify genotyping. *Am. J. Med. Genet.* **94**: 214–227.
5. Waterham, H. R. 2002. Inherited disorders of cholesterol biosynthesis. *Clin. Genet.* **61**: 393–403.
6. Sikora, D. M., K. Pettit-Kekel, J. Penfield, L. S. Merckens, and R. D. Steiner. 2006. The near universal presence of autism spectrum disorders in children with Smith-Lemli-Opitz syndrome. *Am. J. Med. Genet. A.* **140**: 1511–1518.
7. Porter, F. D., and G. E. Herman. 2011. Malformation syndromes caused by disorders of cholesterol synthesis. *J. Lipid Res.* **52**: 6–34.
8. Kelley, R. I., and R. C. Hennekam. 2000. The Smith-Lemli-Opitz syndrome. *J. Med. Genet.* **37**: 321–335.
9. Porter, F. D. 2003. Human malformation syndromes due to inborn errors of cholesterol synthesis. *Curr. Opin. Pediatr.* **15**: 607–613.
10. Bukelis, I., F. D. Porter, A. W. Zimmerman, and E. Tierney. 2007. Smith-Lemli-Opitz syndrome and autism spectrum disorder. *Am. J. Psychiatry.* **164**: 1655–1661.
11. Charman, C. R., A. Ryan, R. M. Tyrrell, A. D. Pearse, C. F. Arlett, H. A. Kurwa, G. Shortland, and A. Anstey. 1998. Photosensitivity

- associated with the Smith-Lemli-Opitz syndrome. *Br. J. Dermatol.* **138**: 885–888.
12. Xu, L., T. A. Davis, and N. A. Porter. 2009. Rate constants for peroxidation of polyunsaturated fatty acids and sterols in solution and in liposomes. *J. Am. Chem. Soc.* **131**: 13037–13044.
 13. Xu, L., Z. Korade, and N. A. Porter. 2010. Oxysterols from free radical chain oxidation of 7-dehydrocholesterol: product and mechanistic studies. *J. Am. Chem. Soc.* **132**: 2222–2232.
 14. Xu, L., Z. Korade, D. A. Rosado, W. Liu, C. R. Lamberson, and N. A. Porter. 2011. An oxysterol biomarker for 7-dehydrocholesterol oxidation in cell/mouse models for Smith-Lemli-Opitz syndrome. *J. Lipid Res.* **52**: 1222–1233.
 15. Xu, L., W. Liu, L. G. Sheflin, S. J. Fliesler, and N. A. Porter. 2011. Novel oxysterols observed in tissues and fluids of AY9944-treated rats - a model for Smith-Lemli-Opitz Syndrome. *J. Lipid Res.* **52**: 1810–1820.
 16. Korade, Z., L. Xu, K. Mirnics, and N. A. Porter. 2013. Lipid biomarkers of oxidative stress in a genetic mouse model of Smith-Lemli-Opitz syndrome. *J. Inherit. Metab. Dis.* **36**: 113–122.
 17. Schroepfer, G. J., Jr. 2000. Oxysterols: modulators of cholesterol metabolism and other processes. *Physiol. Rev.* **80**: 361–554.
 18. Vejux, A., and G. Lizard. 2009. Cytotoxic effects of oxysterols associated with human diseases: Induction of cell death (apoptosis and/or oncosis), oxidative and inflammatory activities, and phospholipidosis. *Mol. Aspects Med.* **30**: 153–170.
 19. Brown, A. J., and W. Jessup. 2009. Oxysterols: sources, cellular storage and metabolism, and new insights into their roles in cholesterol homeostasis. *Mol. Aspects Med.* **30**: 111–122.
 20. Korade, Z., L. Xu, R. Shelton, and N. A. Porter. 2010. Biological activities of 7-dehydrocholesterol-derived oxysterols: implications for Smith-Lemli-Opitz syndrome. *J. Lipid Res.* **51**: 3259–3269.
 21. Xu, L., K. Mirnics, A. B. Bowman, W. Liu, J. Da, N. A. Porter, and Z. Korade. 2012. DHCEO accumulation is a critical mediator of pathophysiology in a Smith-Lemli-Opitz syndrome model. *Neurobiol. Dis.* **45**: 923–929.
 22. Korade, Z., A. K. Kenworthy, and K. Mirnics. 2009. Molecular consequences of altered neuronal cholesterol biosynthesis. *J. Neurosci. Res.* **87**: 866–875.
 23. Albro, P. W., J. T. Corbett, and J. L. Schroeder. 1994. Doubly allylic hydroperoxide formed in the reaction between sterol 5,7-dienes and singlet oxygen. *Photochem. Photobiol.* **60**: 310–315.
 24. Qian, X., Q. Shen, S. K. Goderie, W. He, A. Capela, A. A. Davis, and S. Temple. 2000. Timing of CNS cell generation: a programmed sequence of neuron and glial cell production from isolated murine cortical stem cells. *Neuron.* **28**: 69–80.
 25. Miller, F. D., and A. S. Gauthier. 2007. Timing is everything: making neurons versus glia in the developing cortex. *Neuron.* **54**: 357–369.
 26. Correa-Cerro, L. S., C. A. Wassif, L. Kratz, G. F. Miller, J. P. Munasinghe, A. Grinberg, S. J. Fliesler, and F. D. Porter. 2006. Development and characterization of a hypomorphic Smith-Lemli-Opitz syndrome mouse model and efficacy of simvastatin therapy. *Hum. Mol. Genet.* **15**: 839–851.
 27. Bodin, K., L. Bretillon, Y. Aden, L. Bertilsson, U. Broome, C. Einarsson, and U. Diczfalusy. 2001. Antiepileptic drugs increase plasma levels of 4beta-hydroxycholesterol in humans: evidence for involvement of cytochrome p450 3A4. *J. Biol. Chem.* **276**: 38685–38689.
 28. Bodin, K., U. Andersson, E. Rystedt, E. Ellis, M. Norlin, I. Pikuleva, G. Eggertsen, I. Bjorkhem, and U. Diczfalusy. 2002. Metabolism of 4 beta -hydroxycholesterol in humans. *J. Biol. Chem.* **277**: 31534–31540.
 29. Watabe, T., and T. Sawahata. 1979. Biotransformation of cholesterol to cholestane-3beta,5alpha,6beta-triol via cholesterol alpha-epoxide (5alpha,6alpha-epoxycholestan-3beta-ol) in bovine adrenal cortex. *J. Biol. Chem.* **254**: 3854–3860.
 30. Watabe, T., M. Kanai, M. Isobe, and N. Ozawa. 1981. The hepatic microsomal biotransformation of delta 5-steroids to 5 alpha, 6 beta-glycols via alpha- and beta-epoxides. *J. Biol. Chem.* **256**: 2900–2907.
 31. Aringer, L., and P. Eneroth. 1974. Formation and metabolism in vitro of 5,6-epoxides of cholesterol and beta-sitosterol. *J. Lipid Res.* **15**: 389–398.
 32. Pulfer, M. K., and R. C. Murphy. 2004. Formation of biologically active oxysterols during ozonolysis of cholesterol present in lung surfactant. *J. Biol. Chem.* **279**: 26331–26338.
 33. Song, W., J. Chen, W. L. Dean, R. N. Redinger, and R. A. Prough. 1998. Purification and characterization of hamster liver microsomal 7alpha-hydroxycholesterol dehydrogenase. Similarity to type I 11beta-hydroxysteroid dehydrogenase. *J. Biol. Chem.* **273**: 16223–16228.
 34. Yin, H., L. Xu, and N. A. Porter. 2011. Free radical lipid peroxidation: mechanisms and analysis. *Chem. Rev.* **111**: 5944–5972.
 35. Chesterton, C. J. 1968. Distribution of cholesterol precursors and other lipids among rat liver intracellular structures. *J. Biol. Chem.* **243**: 1147–1151.
 36. Xu, L., L. G. Sheflin, N. A. Porter, and S. J. Fliesler. 2012. 7-Dehydrocholesterol-derived oxysterols and retinal degeneration in a rat model of Smith-Lemli-Opitz syndrome. *Biochim. Biophys. Acta.* **1821**: 877–883.